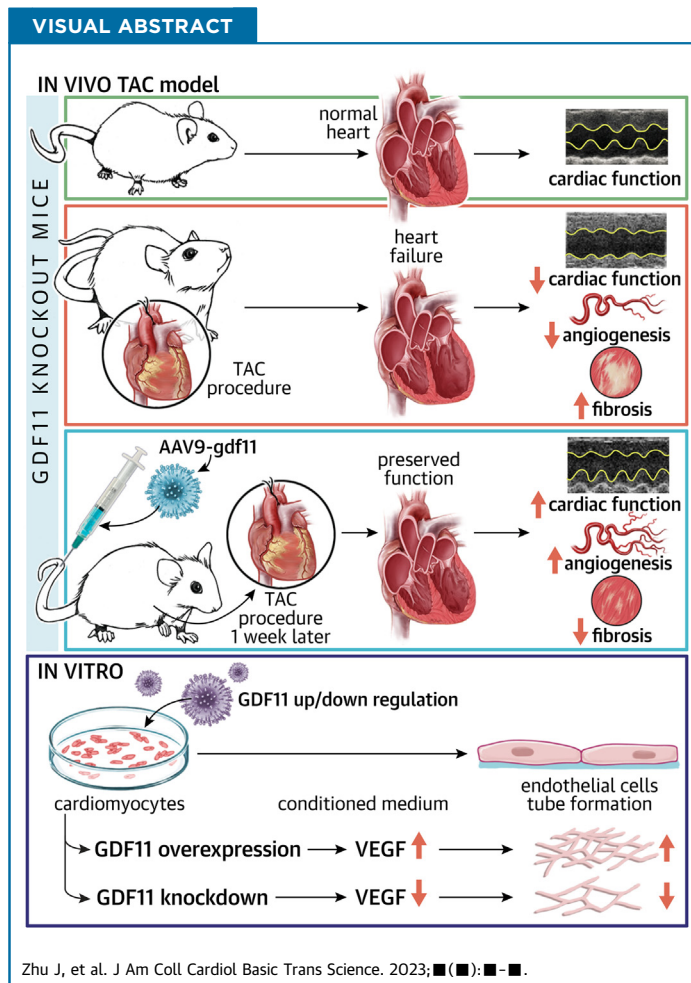


PRECLINICAL RESEARCH

Deficiency of GDF-11 Accelerates TAC-Induced Heart Failure by Impairing Cardiac Angiogenesis

Jinyun Zhu, MD, PhD,^{a,b,*} Ning Zhang, MD, PhD,^{a,c,*} Yun Zhao, MD, PhD,^{d,*} Qi Liu, MD, PhD,^e Yingchao Wang, MD, PhD,^f Mingyao Chen, MD, PhD,^{a,b} Qunchao Ma, MD, PhD,^{a,b} Aiqiang Dong, MD, PhD,^g Yaping Wang, MD, PhD,^{a,b} Hong Yu, MD, PhD^{a,b}

**HIGHLIGHTS**

- Lack of GDF-11 does not influence the heart development and physiological growth.
- However, GDF-11 deficient in cardiomyocytes leads to cardiac remodeling and eventually heart failure under pressure overload.
- GDF-11 acts as an autocrine/paracrine factor to regulate the local cardiac function through promoting angiogenesis via the Akt/mTOR pathway.
- Maintaining GDF-11 homeostasis in the heart improves and rescues contractile dysfunction following pressure overload.

From the ^aDepartment of Cardiology, Second Affiliated Hospital, College of Medicine, Zhejiang University, Hangzhou, China; ^bCardiovascular Key Laboratory of Zhejiang Province, Hangzhou, China; ^cDepartment of Cardiology, Affiliated Hangzhou First People's Hospital, College of Medicine, Zhejiang University, Hangzhou, China; ^dDepartment of Ultrasound, Second Affiliated Hospital of Shandong First Medical University, Taian, China; ^eDepartment of Cardiology, Sir Run Run Shaw Hospital, School of

ABBREVIATIONS AND ACRONYMS

AAV9 = adeno-associated virus serotype 9

ACM = adult ventricular cardiomyocyte

ActR = activin receptor

ALK = activin receptor-like kinase

ANP = atrial natriuretic peptide

BNP = B-type natriuretic peptide

CKO = cardiomyocyte-specific knockout

CM = cardiomyocyte

cTnT-Cre = cardiac troponin T-Cre

DCM = dilated cardiomyopathy

EC = endothelial cell

ELISA = enzyme-linked immunosorbent assay

GDF = growth differentiation factor

HUVEC = human umbilical vein endothelial cell

mRNA = messenger RNA

NC = negative control

NKO = Nkx2.5-Cre knockout

NMCM = neonatal mouse cardiomyocyte

p-Akt = phosphorylated Akt

PE = phenylephrine

rGDF = recombinant growth differentiation factor

SERCA2a = sarco(endo)plasmic reticulum calcium adenosine triphosphatase 2a

shNC = negative control short hairpin RNA

siGDF = short hairpin RNA targeting mouse growth differentiation factor

shRNA = short hairpin RNA

siGDF = small interfering RNA targeting mouse growth differentiation factor

siNC = scrambled control small interfering RNA

siRNA = small interfering RNA

SIS3 = Smad3 inhibitor

TAC = transverse aortic constriction

TGF = transforming growth factor

TKO = cTnT-Cre knockout

VEGF = vascular endothelial growth factor

SUMMARY

The role of growth differentiation factor (GDF)-11 in cardiac diseases has not been fully determined. Our study revealed that GDF-11 is not essential for myocardial development and physiological growth, whereas its absence exacerbates heart failure under pressure overload condition via impairing the responsive angiogenesis. GDF-11 induced VEGF expression in CMs by activating the Akt/mTOR pathway. The effect of endogenous GDF-11 on the heart belongs to local self-regulation of myocardial tissue, rather than a way of systemic regulation. (J Am Coll Cardiol Basic Trans Science 2023; ■: ■-■) © 2023 Published by Elsevier on behalf of the American College of Cardiology Foundation. This is an open access article under the CC BY-NC-ND license (<http://creativecommons.org/licenses/by-nc-nd/4.0/>).

Cardiac hypertrophy can be induced by the increased external loads that are caused by cardiovascular events, such as hypertension, aortic stenosis, and myocardial infarction. Such cardiac hypertrophy with preserved contractility initially might be compensatory and adaptive. However, if hypertrophy progresses pathologically, it can be deleterious, inducing decompensation and dysfunction, and ultimately result in heart failure and sudden death.¹ Understanding the molecular mechanisms of cardiac hypertrophy is essential to protect myocardium from pathological remodeling and slow down the progression of heart failure.² The secretomes produced by the heart encompass a group of proteins that have been referred to as cardiokines. The most well-established heart-derived hormones are atrial natriuretic peptide (ANP) and B-type natriuretic peptide (BNP), discovered almost 40 years ago.³ Recent research has identified other heart-derived hormones, such as growth differentiation factor (GDF)-15, GDF-8, and activin A.⁴ These secreted proteins are required for the maintenance of normal cardiac function, and they control pathological remodeling of the myocardium in response to injury in an autocrine and/or paracrine ways.⁵ Given the crit-

ical role of cardiokines in heart disease, they might represent a promising therapeutic target.

GDF-11 is a secreted protein that is highly related to GDF-8. Both belong to the transforming growth factor (TGF)- β superfamily. GDF-11 has been identified as a critical factor for axial patterning, organogenesis development such as in kidney and pancreas, and neuronal development.⁶ Recently, GDF-11 was shown to rejuvenate cardiac function, improve cerebral vasculature perfusion, and promote neurogenesis in old mice.⁷⁻⁹ However, some other results did not support these conclusions and demonstrated that increasing GDF-11 levels inhibited skeletal muscle regeneration¹⁰ and had no effect on aging and cardiac hypertrophy.¹¹ The role of GDF-11 in aging and heart diseases has been highly controversial due to the conflicting reports about its circulating levels and limited information regarding its functional consequences in the heart in vivo. It is known that both GDF-8¹² and GDF-11 negatively regulate skeletal muscle mass.¹³⁻¹⁵ Conditional GDF-8 knockout in the adult murine heart leads to abnormal glycogen metabolism, heart failure, and increased lethality.¹⁶ Whether GDF-11 has a similar negative effect on myocardium as GDF-8 is still unknown.

Previous studies have focused on the active forms of GDF-11 in circulation, rather than on tissue-specific expression and local effects.^{9,17} Most of this research restored youthful levels of GDF-11 in circulation by injecting recombinant growth differentiation factor

Medicine, Zhejiang University, Hangzhou, China; ^fPharmaceutical Informatics Institute, College of Pharmaceutical Sciences, Zhejiang University, Hangzhou, China; and the ^gDepartment of Cardiovascular Surgery, Second Affiliated Hospital, College of Medicine, Zhejiang University, Hangzhou, China. *Drs Zhu, Zhang, and Zhao contributed equally to this work.

The authors attest they are in compliance with human studies committees and animal welfare regulations of the authors' institutions and Food and Drug Administration guidelines, including patient consent where appropriate. For more information, visit the [Author Center](#).

Manuscript received August 31, 2021; revised manuscript received November 21, 2022, accepted November 22, 2022.

(rGDF)-11 into old mice.^{9,15,18,19} The different dose and biological activity of rGDF11 may contribute to the opposite results. Although it is well recognized that GDF-11 is expressed widely in different tissues, little is known about its effect in specific tissue. Understanding the effect of GDF-11 for cardiac functions, especially under pathological conditions, would uncover the potentially distinct roles of GDF-11 in the heart. In the present study, we demonstrated that GDF-11 largely functions in an autocrine or paracrine manner to regulate local cardiac function.

METHODS

An expanded version of the Methods section, including detailed experimental procedures on animals, a list of polymerase chain reaction primers and antibodies, is presented in the [Supplemental Appendix](#).

HUMAN MYOCARDIAL TISSUE. Heart tissue samples were collected from heart recipient patients undergoing heart transplantation (mean age 52 ± 4 years) ([Supplemental Table 1](#)). They were diagnosed as dilated cardiomyopathy (DCM) revealed by echocardiography and/or posttransplantation pathological examination. Normal heart tissues as the control group were obtained from patients who died from noncardiac reasons (mean age 48.00 ± 5.52 years). The collection and use of human heart tissues were approved by the Human Research Ethics Committee of the Second Affiliated Hospital, Zhejiang University School of Medicine. All recipients and each donor's family members signed informed consent forms.

GENERATION OF KNOCKOUT MICE. All animal experiments were performed under the approval of the Animal Ethics Committee of Zhejiang University, which complies with the Guide for the Care and Use of Laboratory Animals, eighth edition, published by the U.S. National Institutes of Health. Mice containing a pair of loxP sites flanking exon 2 of GDF-11 were generated at the Shanghai Bio Model Organisms Center. GDF-11^{fl/ox} mice were crossed with cardiomyocyte (CM)-specific inducible Cre mice (Myh6-MerCreMer) to create Myh6-MerCreMer/GDF-11^{fl/fl} (hereafter referred to as cardiomyocyte-specific knockout [CKO]) mice for at least 6 generations before use. Cre recombination was achieved by intraperitoneal administration of tamoxifen every other day for 5 times (250 mg/kg) at mice 4 to 6 weeks after birth, with a 3-week rest after tamoxifen use. GDF-11^{fl/fl} mice were also crossed with Nkx2.5-Cre and

cardiac troponin T-Cre (cTnT-Cre) to generate Nkx2.5-Cre/GDF-11^{fl/fl} and cTnT-Cre/GDF-11^{fl/fl} embryos, respectively (hereafter referred to as NKO and TKO). All animals were with C57/BL6/J background, only male mice were used.

SURGICAL PROCEDURES. Mice (9-12 weeks old, 20-25 g weight) were anesthetized by intraperitoneal injection of 100 mg/kg ketamine combined with 10 mg/kg xylazine and ventilated via tracheal intubations connected to a rodent ventilator. Transverse aortic constriction (TAC) surgery was performed to induce cardiac hypertrophy using a 26-gauge needle as described previously,²⁰ while the sham group underwent the same procedure without aorta constriction. For the mice injected with adeno-associated virus serotype 9 (AAV9) through the tail vein, TAC was conducted 1 week later using a 26-gauge needle.

ECHOCARDIOGRAPHY. Transthoracic 2-dimensional M-mode echocardiography was used to measure left ventricular ejection fraction, left ventricular fractional shortening, and end-diastolic left ventricular internal diameter with Vevo 2100 system (VisualSonics). This procedure was repeated 3 times with use of the same equipment by the same examiner.

HISTOLOGICAL ANALYSIS. Hearts were arrested with 1% KCl and fixed in 10% formalin. The fixed hearts were embedded in paraffin and sectioned into 5- μ m slices, which were stained with hematoxylin and eosin for histological analysis or with Picrosirius Red for collagen examination. Wheat germ agglutinin (Sigma-Aldrich) was used to visualize cellular membranes and measure the cross-sectional area of myocytes. Image-Pro Plus software (version 6.0; Meyer Instruments) was used to analyze myocytes.

QUANTIFICATION OF GDF-11, GDF-8, AND ACTIVIN A IN SERUM. GDF-11, GDF-8, and activin A levels in mouse serum and conditioned medium were measured by GDF-11 enzyme-linked immunosorbent assay (ELISA) (SEC 113Mu-96T, Cloud-Clone), GDF-8 ELISA (SEKM-0158-Mu-96T, Solarbio), and activin A ELISA assay (SEKM-0231-Mu-48T, Solarbio), according to the manufacturer's instructions, respectively.

CELL ISOLATION AND CULTURE. Adult ventricular cardiomyocytes (ACMs) were isolated from adult mice described previously.²¹ Neonatal mouse/rat ventricular CMs were isolated from 1-day-old C57BL/6J mice or Sprague-Dawley rats. Neonatal mouse cardiomyocyte (NMCM) hypertrophy was induced with phenylephrine (PE) (50 μ M) for 24 hours, and cell size

was determined by measuring cell surface area, hypertrophic, and fibrotic markers. CMs were cultured in serum-free medium for 6 hours and then stimulated separately with 50 ng/mL rGDF-11 for 24 hours, 1 μ M inhibitor of activin receptor-like kinase (ALK) SB431542 for 24 hours, and 1 μ M SB431542 for 24 hours after GDF-11 stimulation or 10 μ M Akt inhibitor MK 2206 for 24 hours (Selleckchem).

GDF11 OVEREXPRESSION AND ITS KNOCKDOWN.

Overexpression of GDF-11 in CMs (CM^{GDF11}) was achieved by transduction of lentiviral vector carrying GDF-11 gene (GDF-11), and the negative control (NC) was CMs that had only been exposed to the lentiviral vector. CMs were mixed with the lentiviral vector at the multiplicities of infection of 50 with polybrene (final concentration of 8 μ g/mL, Sigma-Aldrich).

Both small interfering RNA (siRNA) and short hairpin RNA (shRNA) were used to decrease GDF-11 expression. The small interfering RNA targeting mouse growth differentiation factor (siGDF)-11 and the scrambled control small interfering RNA (siNC) were purchased from GenePharma. For knockdown of GDF-11, CMs were transfected with either siGDF11 or siNC (50 nM) using lipofectamine 2000 transfection reagent (Invitrogen). Adenoviral vector expressing shRNA targeting mouse GDF-11 (shGDF-11) and Ad-sh-Vector (shNC) were constructed and packaged by Vigene Biosciences. CMs were transduced with shGDF-11 or shNC (multiplicities of infection = 200) according to the manufacturer's instructions.

TUBE FORMATION AND NEUTRALIZATION ASSAY.

Conditioned medium of neonatal mouse/rat ventricular CMs was collected and concentrated 10-fold using Microcon (Millipore) to culture human umbilical vein endothelial cells (HUVECs) for tube formation assay. At specific condition, TGF- β type I receptor inhibitor SB431542 (1 μ M) or Smad3 inhibitor (SIS3) (3 nM) was added into the medium 24 hours prior to medium change. The medium was replaced with fresh Dulbecco's modified Eagle medium (DMEM) without serum. After being cultured for another 24 hours, the supernatants were collected and concentrated. Vascular endothelial growth factor (VEGF) in the concentrated medium was determined using a commercial ELISA kit. Goat Anti-Mouse VEGF₁₆₄ Antigen Affinity-purified Polyclonal Antibody (Catalog #AF-493-NA) or rabbit IgG (sc-2027, 4 μ g/mL final concentration, Santa Cruz Biotechnology) as a control treatment was added to the conditioned medium of CMs to neutralize VEGF during the tube formation assay of HUVECs.

RNA SEQUENCING AFTER KNOCKDOWN GDF-11.

Total RNA was extracted from CMs using TRIzol (Life Technologies) after NMCMs were transfected with shGDF-11 and shNC for 48 hours. Preparation of library and sequencing of transcriptome were carried out using Illumina novaseq (Novogene Bioinformatics Technology). Differential expression analysis of 2 conditions (3 biological replicates per condition) was performed using the DESeq2 R package (DESeq2 (1.16.1), edgeR (3.18.1); R Foundation for Statistical Computing). Genes with an adjusted *P* value <0.05 found by DESeq2 were assigned as differentially expressed. RNA sequencing data are deposited in Gene Expression Omnibus datasets with accession number (GSE182423).

GENERATION AND ADMINISTRATION OF AAV9 VECTORS. The AAV9 carrying GDF-11 was constructed and packaged by Vigene Biosciences.

The coding sequence of mouse GDF-11 was synthesized and cloned into AAV9-cTnT-Myc plasmid. A different dose of AAV9 viral particles (low dose 4×10^{11} , mild dose 3×10^{12} , high dose 7×10^{12} /viral particles/mouse) was injected through tail vein. One week post-AAV9 injection, TAC surgery was performed, and the mice were observed for 56 days.

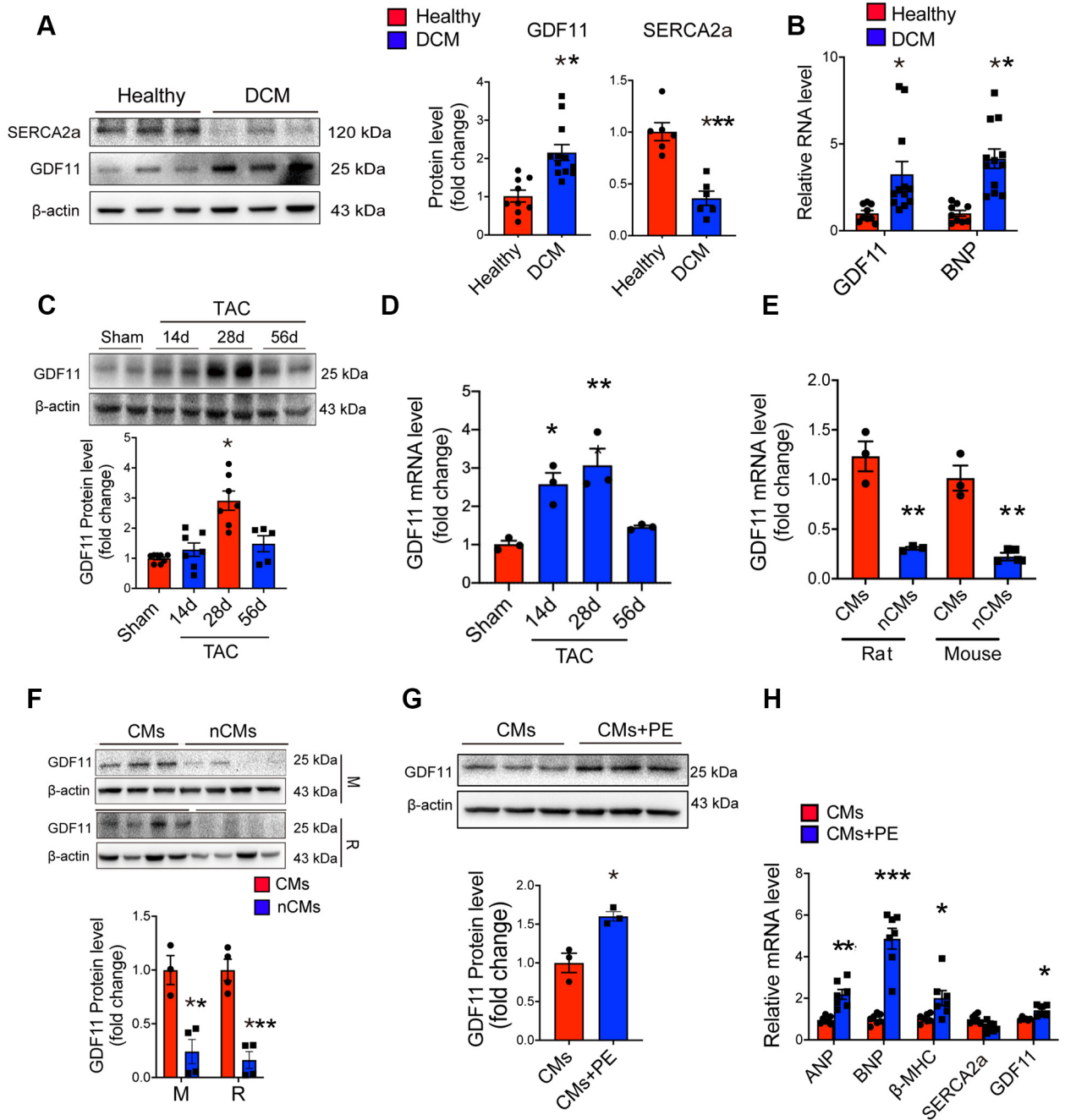
STATISTICAL ANALYSIS. All data are presented as the mean \pm SEM. Statistical analyses were performed with Prism 8 (GraphPad Software). Continuous variables were compared by *t* test. The comparison of 2 or more groups was performed by 1- or 2-way analysis of variance (analysis of variance with Bonferroni's post hoc test for multiple pairwise comparisons). Kaplan-Meier methods were used for survival analysis (log-rank test). A 2-tailed *P* value lower than 0.05 indicated statistical significance.

DATA AVAILABILITY STATEMENT. The data that support the findings of this study are available from the corresponding author upon reasonable request.

RESULTS

GDF-11 EXPRESSION WAS INCREASED IN STRESSED HEARTS.

To explore the role of GDF-11 in pathological cardiac conditions, GDF-11 expression in human hearts were measured. GDF-11 at the protein level was significantly higher in DCM hearts in comparison with that in normal hearts (Figure 1A), accompanied by decreased expression of Sarco(endo)plasmic reticulum calcium adenosine triphosphatase 2a (SERCA2a), which is a reflection of cardiac dysfunction. GDF-11 at the messenger RNA (mRNA) level was also increased

FIGURE 1 GDF11 Expression Is Upregulated in Stressed Hearts and Is Mainly Produced by CMs

(A) Representative Western blot and quantitation of growth differentiation factor (GDF)-11 and sarco(endo)plasmic reticulum calcium adenosine triphosphatase 2a (SERCA2a) protein in the heart from healthy and dilated cardiomyopathy (DCM) patients ($n = 12$ for DCM; $n = 9$ for healthy patient GDF-11 level and $n = 6$ for healthy patient SERCA2a level). **(B)** The relative levels of GDF-11 messenger RNA (mRNA) in healthy and DCM hearts ($n = 12$ for DCM patients, $n = 9$ for healthy patients). Values represent the fold changes relative to the donors. The actin mRNA level was used as the internal control. **(C)** Representative Western blot and quantitation of GDF-11 protein in mouse hearts after sham surgery and 14, 28, and 56 days after transverse aortic constriction (TAC) ($n = 8$ for sham, $n = 7$ for TAC 14 days and TAC 28 days, $n = 5$ for TAC 56 days). **(D)** The relative levels of GDF11 mRNA in sham and TAC hearts ($n = 3$ for sham and TAC). Values represent the fold changes relative to the sham. The actin mRNA level was used as the internal control. **(E)** Quantification of GDF11 mRNA (normalized to actin mRNA) from cardiomyocytes (CMs) and noncardiomyocytes (nCMs) isolated from rat or mouse hearts 1 day after birth ($n = 3$). **(F)** Immunoblot and quantitation of GDF11 protein in mouse (**top**) and rat (**bottom**) ($n = 3$). **(G)** Immunoblot and quantification for GDF11 in control and 50 μ M phenylephrine (PE)-treated neonatal mouse CMs. β -actin was the loading control ($n = 3$). **(H)** Quantification of GDF11 and hypertrophic gene marker mRNA (normalized to actin mRNA) from CMs with or without 50 μ M PE ($n = 7$ for atrial natriuretic peptide [ANP], B-type natriuretic peptide [BNP], β -myosin heavy chain [β -MHC], and SERCA2a; $n = 6$ for GDF11). * $P < 0.05$, ** $P < 0.01$ and *** $P < 0.001$ vs healthy donors or CMS or sham. M = mouse; R = rat.

in DCM hearts (Figure 1B). Confirmed by immunohistochemistry, myocardia from DCM have more collagen deposition (Supplemental Figure 1A). Consistent with the results in human, GDF-11 expression in mouse hearts was significantly increased after TAC surgery, the peak point was 4-fold higher than the control at 28-day post-TAC (Figures 1C and 1D). These findings indicated that GDF-11 expression in the heart was increased under pathological stress.

In order to identify the source of GDF-11 in hearts, we separated CMs from non-CM cells in hearts and found that GDF-11 was mainly enriched in CMs from either neonatal mice (Figures 1E and 1F) or adult mice (Supplemental Figure 1B). GDF-11 in CMs was also significantly increased when CMs were cultured either with hypertrophic agonists PE (Figures 1G and 1H; Supplemental Figure 1C) or under hypoxia conditions (Supplemental Figures 1D and 1E) to mimic hypertrophic or hypoxia stress, respectively.

Because activin A and GDF-8 also act as activin receptor II (ActRII) ligands, their mRNA and circulating levels were also evaluated at various time points with or without TAC. Similar to GDF-11, activin A transcript levels were elevated in the heart at 14 days after TAC (Supplemental Figure 2A). However, circulating GDF-11 and GDF-8 levels had no change after TAC surgery (Supplemental Figure 2B).

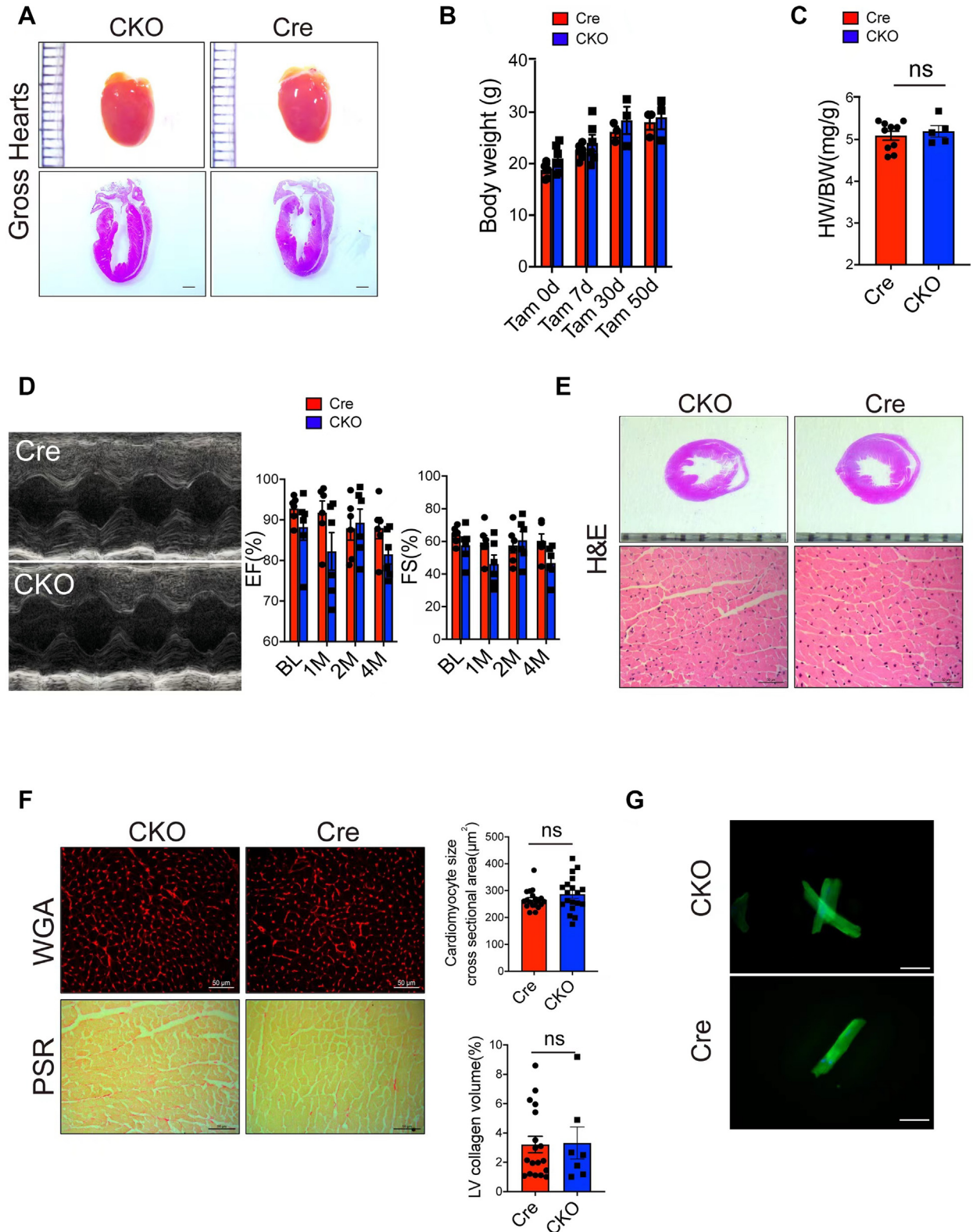
GDF-11 DEFICIENCY IN CMs RESULTED IN NO APPARENT CARDIAC ABNORMALITIES. To investigate the role of GDF-11 in cardiac function, an inducible CKO mouse (Myh6Cre⁺/GDF-11^{fl/fl}) was created to study whether GDF-11 deficiency accelerates the cardiac dysfunction in vivo (Supplemental Figure 3). No abnormality of gross heart morphology (Figure 2A) and body weight (Figure 2B) was observed for the CKO mice. The heart weight and normal cardiac function (Figures 2C and 2D) were similar between CKO mice and control littermates. The size of CMs and fibrosis volume in the hearts were not significantly different between 2 groups (Figures 2E and 2F). In order to further clarify the effect of GDF-11 deletion on the cellular level, we isolated adult CMs from Cre (ACM^{Cre}) and CKO (ACM^{CKO}) mice and found no obvious difference in cell morphology between 2 groups (Figure 2G). For up to 18-month long-term observation, there was no significant heart dilation and age-related ventricular hypertrophy measured by cross-sectional ventricular diameter and CM size for CKO mice as compared with Cre mice (Supplemental Figures 4A to 4C). The density of CD31-positive capillaries was also similar between 2

groups (Supplemental Figure 4D). There were no significant differences in the expression of connective tissue growth factor and Col1a (collagen 1a) between the 2 groups (Supplemental Figure 4E).

To assess the role of GDF-11 in ACM excitation-contraction coupling, ACM contractility and Ca²⁺ transients were compared between ACM^{Cre} and ACM^{CKO}. There were no significant differences in the magnitude of electrically evoked Ca²⁺, time to peak, time of Ca²⁺ transient decay, fractional shortening, and the time to peak shortening between ACM^{Cre} and ACM^{CKO} (Supplemental Figures 5A and 5B). These findings indicate that GDF-11 deficiency in CMs did not affect cellular contractility and Ca²⁺ handling.²²

In order to identify whether cardiac-specific GDF-11 deficient affects embryonic survival and cardiac morphology, mice with CM-specific ablation of GDF-11 at the embryonic stage were produced using Nkx2.5-driven Cre (NKO) and cTnT-Cre (TKO). NKO mice were viable with normal heart structure, function, and cardiac morphology (Supplemental Figures 6A to 6C) and showed no significant differences in the density of CD31-positive capillary and size of CMs as compared with the control group (Supplemental Figures 6D and 6E). Circulating levels of GDF-11 were also similar between 2 groups (Supplemental Figure 6F). Heart structure and cardiac morphology in TKO mice were also similar to their littermates (data not shown). These results demonstrated that endogenous GDF-11 in CMs is not essential for myocardial development and physiological growth.

GDF-11 DEFICIENCY IN CMs CAUSED HEART SUSCEPTIBLE TO CARDIAC DYSFUNCTION AFTER TAC. To explore whether GDF-11 could regulate pathological progression, heart structure and function were compared between CKO and Cre mice after TAC surgery (Supplemental Figure 7A). CKO mice manifested more pronounced cardiac dysfunction and dilation than the control mice at 46 days post-TAC (Figures 3A and 3B). Increased heart weight-to-body weight and heart weight-to-tibial length ratios were observed in CKO mice as compared with the control mice at 46 days post-TAC (Figure 3C). The death rate of CKO mice was higher than that of control mice post-TAC (Supplemental Figure 7B). TAC-induced enlargement of CMs was significantly more severe in CKO mice than the control mice at 46 days post-TAC (Figure 3D). More fibrosis in both interstitial and perivascular areas was observed (Figure 3E). Increased ANP, a heart failure marker, was detected in the hearts from CKO mice in comparison with the control mice

FIGURE 2 Lack of CM GDF-11 Does Not Affect Cardiac Function

(Figure 3F). Hemodynamic measurements at 46 days post-TAC showed that CKO mice exhibited significantly reduced $-dp/dt$ (left ventricular pressure drop rate) in response to TAC (Figure 3G), indicating impaired cardiac function. More serious mitochondria disorganization and sarcomere disarray were observed in the heart tissues of CKO mice post-TAC (Supplemental Figure 7C). These data demonstrated that CKO mice were more vulnerable to develop decompensated heart failure when cardiac stress occurred.

GDF-11 DEFICIENCY WEAKENED REPARATIVE ANGIOGENESIS IN THE HEART AFTER PRESSURE OVERLOAD. Impaired angiogenesis has been shown to drive cardiac from hypertrophy to failure.^{23,24} To determine the role of GDF-11 on cardiac angiogenesis, capillary density (CD31+) per CMs and matured vasculature (α -smooth muscle actin) in the hearts 14 to 56 days post-TAC were evaluated (Supplemental Figure 8). CKO mice displayed significant lower capillary density in their hearts 56 days post-TAC (Figure 4A). At the earlier stage (14 and 28 days post-TAC), a slightly decreased (and not significant) capillary density was observed in the hearts from CKO mice. The matured vasculature was not affected in CKO mice as compared with the control mice (Figure 4B).

It is known that VEGF is induced in stressed myocytes and hearts for adapting to cardiac hypertrophy.²⁵ Significantly less VEGF both in mRNA and protein levels were detected in the hearts of CKO mice as compared with the hearts of in control mice (Figures 4C and 4D). These results demonstrate that deficiency of GDF-11 in CMs leads to a blunted angiogenesis following pressure overload, which possibly leads to an accelerated progression of heart failure.

GDF-11 REGULATED PROANGIOGENIC PARACRINE ACTIVITY IN CMs. To investigate the role of GDF-11 in proangiogenesis, the paracrine effect of CMs on endothelial cells (ECs) was examined. GDF-11 in the

NMCMs was overexpressed by lentiviral transduction with GDF-11 gene (CM^{GDF11}) or knockdown by GDF-11-specific shRNA (CM^{shGDF11}) or siRNA (CM^{siGDF11}). GDF-11 concentration in the conditioned medium was increased in CM^{GDF11} and decreased in CM^{shGDF11} (Supplemental Figure 9A). The reduced GDF-11 production in CM^{shGDF11} could be rescued to a level similar to the control with lentiviral transduction of GDF-11 (CM^{shGDF11+GDF11}) (Supplemental Figure 9B).

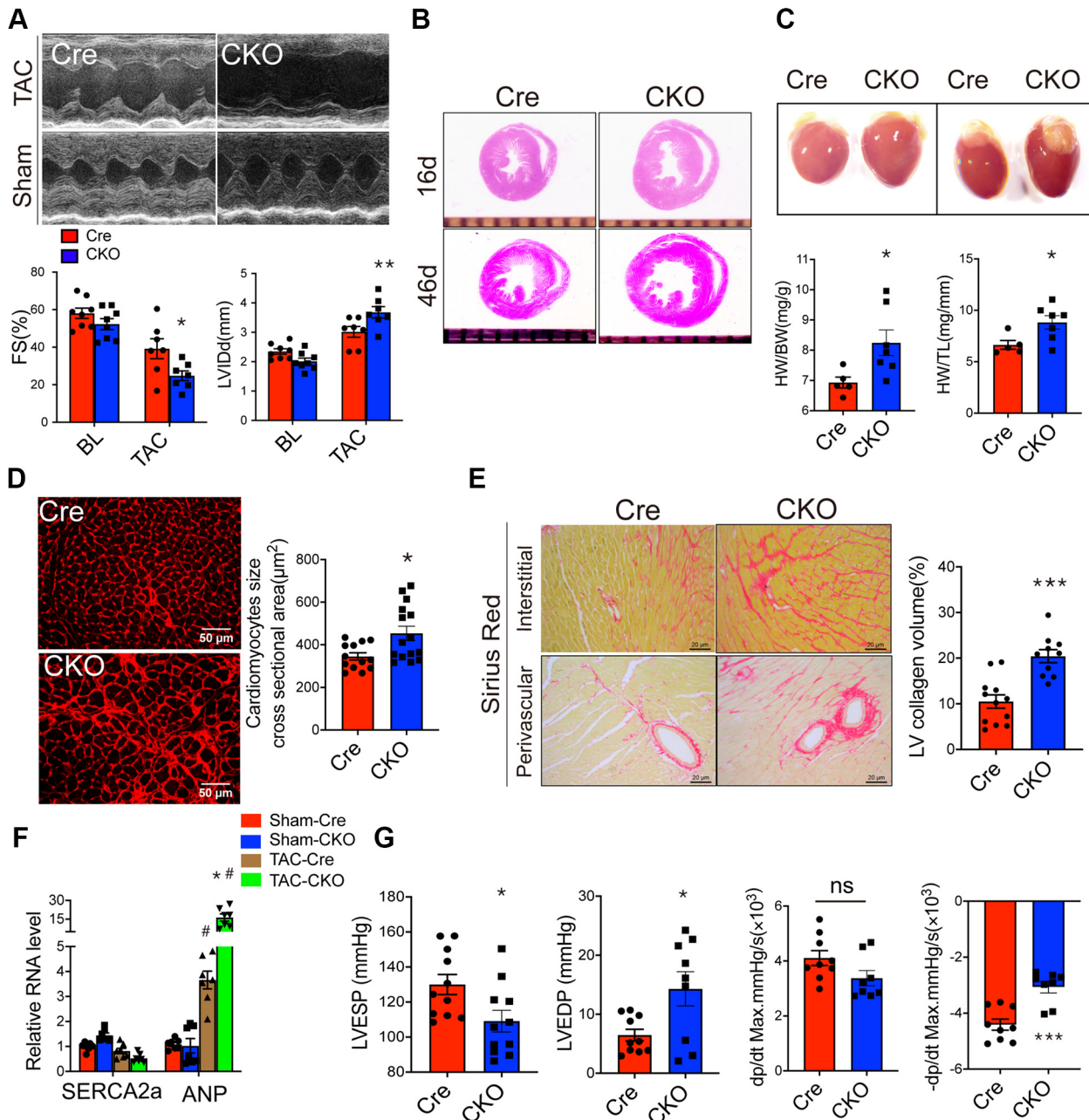
When the conditioned medium from CM^{GDF11} was used to culture HUVECs, the capacity of tube formation of HUVECs was significantly improved. Decreased tube formation was observed when HUVECs were cultured with the conditioned medium from CM^{siGDF11} as compared with the negative control (CM^{NC}), which was reverted when the conditioned medium was derived from CM^{siGDF11} that were transduced with the lentiviral GDF-11 (CM^{siGDF11+GDF11}) (Figure 4E).

RNA-sequencing analysis showed that 3,293 genes were downregulated and 3,214 genes were upregulated in CM^{shGDF11} whose GDF-11 was knocked down (Supplemental Figure 10A). Gene Ontology analysis of these differentially expressed genes indicated that genes related to angiogenesis were among the top down-regulated biological processes (Supplemental Figures 10B and 10C). Marker genes for angiogenesis, such as VEGF, Ang-1, Ang-2, Cdh5, vWF, and PDGF, were significantly reduced in CM^{shGDF11}. These data supported that GDF-11 deficiency in CMs impairs their paracrine effect for angiogenesis and suggested the VEGF pathway as an important part for GDF-11-mediated effect of cardiac protection.

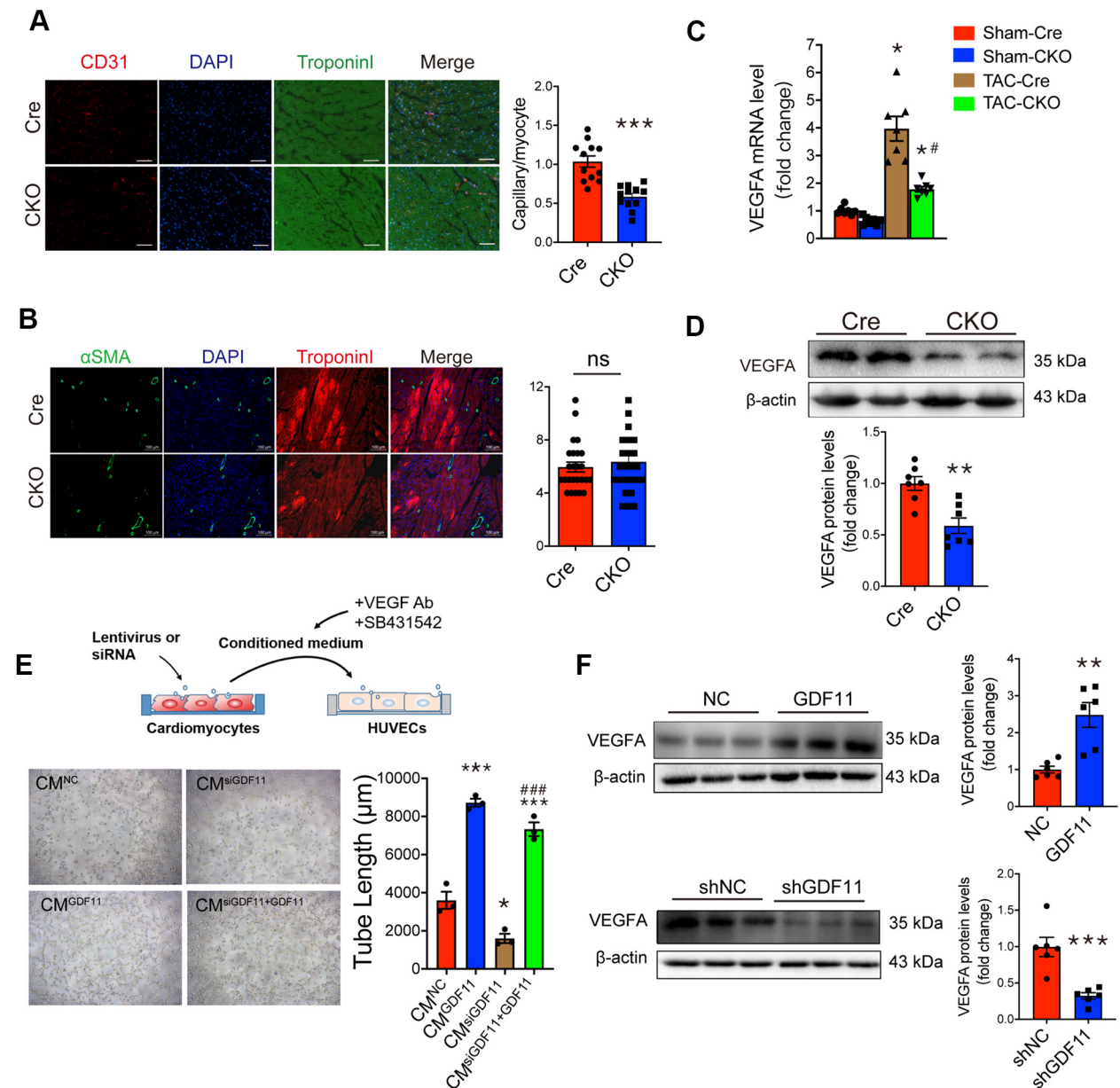
In confirmation, higher VEGF expression both in mRNA and protein levels was detected in CM^{GDF11}, whereas knockdown of GDF-11 in CMs resulted in the opposite effects (Figure 4F, Supplemental Figure 11A). The level of VEGF in the conditioned medium from CM^{GDF11} was also increased compared with control group (CM^{NC}) by ELISA assay (Supplemental Figure 11B). Such an effect of GDF-11 on VEGF expression in CMs was blocked with TGF- β receptor

FIGURE 2 Continued

(A) (Top) Gross morphology of Cre and cardiomyocyte-specific knockout (CKO) hearts (scale bar = 1 mm). (Bottom) Representative hematoxylin and eosin (H&E) stain of longitudinal sectional heart from Cre and CKO mice (scale bar = 1 mm). (B) For both male and female mice, the body weight was measured in CKO and Cre mice (as control animal) after injection of tamoxifen (Tam) at the indicated days (n = 6 for Cre/CKO at Tam 0-7 days, n = 3 for Cre/CKO at Tam 30 -50 days). (C) Heart weight-to-body weight (HW/BW) ratio in Cre and CKO mice at 12 weeks (n = 10 for Cre, n = 5 for CKO). (D) Representative echocardiographic M-mode images of Cre and CKO hearts. Quantification of the ventricular function reflected by ejection fraction (EF) and fractional shortening (FS) for 4 months (n = 6 for Cre, n = 6 for CKO). (E) Representative H&E stain of transverse cross-section and magnification partial image (scale bar = 50 μ m) from Cre and CKO mice at 8 weeks. (F) Representative wheat germ agglutinin (WGA) (scale bar = 50 μ m) and Picrosirius Red (PSR) stain (scale bar = 50 μ m) images of transverse sections from Cre and CKO hearts. Quantification of CM cell area and fibrosis measured in the myocardium of Cre and CKO mice 12 weeks (n > 50 cells/group for CMs area; n = 19). (G) Representative fluorescence images (troponin I [green]) of isolated adult CMs from CKO and Cre mice, respectively (scale bar = 50 μ m). LV = left ventricular; other abbreviations as in Figure 1.

FIGURE 3 GDF11 Deficiency Accelerates the Transition From Compensated Hypertrophy to Heart Failure

(A) Representative images and quantification of echocardiographic FS and left ventricular end-diastolic diameter (LVIDd) of mice treated as described in the indicated groups ($n = 8$ for baseline [BL], $n = 7$ for TAC 46 days). (B) Histological analyses of heart sections stained with H&E from the indicated groups after TAC 16 days and 46 days. (C) Gross morphology of Cre and CKO heart after TAC 46 days. Comparison of the HW/BW and heart weight-to-tibial length (HW/TL) ratios in Cre and CKO mice ($n = 5$ for Cre, $n = 7$ for CKO). (D) Representative images of WGA (scale bar = $50 \mu\text{m}$) from the indicated groups 46 days after TAC. The quantification of average cross-sectional area of CMs in the indicated groups were shown in bar graph ($n > 50$ cells/group for CM area; $n = 13$ for Cre, $n = 15$ for CKO). (E) Interstitial and perivascular Sirius red staining (scale bar = $20 \mu\text{m}$) was performed to determine cardiac fibrosis of the hearts from CKO and Cre mice after TAC 46 days. Quantification of cardiac collagen volume in the indicated groups ($n = 12$ for Cre, $n = 10$ for CKO). (F) Quantitative reverse-transcriptase polymerase chain reaction was performed to analyze the mRNA levels of SERCA2a and ANP genes ($n = 7$) in the post-TAC CKO and Cre mice. (G) The hemodynamics results of left ventricular end-systolic pressure (LVESP), left ventricular end-diastolic pressure (LVEDP), and \pm left ventricular maximum pressure rise/drop rate from CKO and Cre mice in response to TAC ($n > 6$ for Cre, $n > 6$ for CKO). * $P < 0.05$, ** $P < 0.01$ and *** $P < 0.001$ vs TAC-Cre. # $P < 0.05$ vs sham-Cre. Abbreviations as in Figures 1 and 2.

FIGURE 4 GDF11 Deficiency Causes Decreased Cardiac Angiogenesis and VEGF Expression Following Pressure Overload

(A) Representative immunofluorescent images of heart sections from Cre and CKO mice 56 days post-TAC after staining for CD31 (red), troponin I (green), and DAPI (blue). CD31-positive cells were quantified in the bar graph (scale bar = 50 μ m) ($n = 12$). $***P < 0.001$ vs Cre. **(B)** Representative image of heart sections stained with α -smooth muscle actin (SMA) (green), troponin I (red), and DAPI (blue), and the quantification of α SMA-positive cells (scale bar = 50 μ m) ($n = 25$). **(C)** Quantitative reverse-transcriptase polymerase chain reaction was performed to analyze the mRNA levels of vascular endothelial growth factor (VEGF) genes in the post-TAC CKO and Cre mice ($n = 7$). $*P < 0.05$ vs sham-Cre. $\#P < 0.05$ vs TAC-Cre. **(D)** Immunoblot for the VEGF proteins from hearts of Cre and CKO mice after sham or TAC surgery at 56 days ($n = 7$). $**P < 0.01$ vs Cre. **(E)** Schematic diagram of the primary neonatal mouse CM paracrine experiment. The conditioned medium was concentrated 10-fold and then co-cultured with human umbilical vein endothelial cells (HUVECs) for tube formation. Representative images and quantification of tube formation in HUVECs stimulated by the conditioned medium from CMs overexpressing GDF-11 (CM^{GDF11}) by lentivirus or negative control (CM^{NC}), or CMs transfected with small interfering RNAs (siRNAs) alone (CM^{siGDF11}) or siRNAs followed by overexpressed GDF-11 by lentivirus at 48 hours (CM^{siGDF11+GDF11}) ($n = 3$). $*P < 0.05$, $***P < 0.001$ vs CM^{NC}. $###P < 0.001$ vs CM^{siGDF11}. **(F)** Immunoblot of the VEGF proteins from neonatal mouse CMs after transfection with lentivirus (top) or short hairpin RNA (bottom) for 48 hours. The β -actin was the loading control scenario ($n = 6$). $**P < 0.01$, $***P < 0.001$ vs negative control (NC) scenario or shNC. Ab = antibody; shGDF = short hairpin RNA targeting mouse growth differentiation factor; shNC = negative control short hairpin RNA; other abbreviations as in Figures 1 and 2.

inhibitor SB431542 (Supplemental Figure 11B), indicating the autocrine effect of GDF11 on VEGF expression. When the conditioned medium was collected from CMs in the presence of SB431542, the effect of GDF-11-mediated CM paracrine actions on HUVEC tube formation was abolished (Supplemental Figure 11C), confirming that the autocrine effect of GDF-11 in CMs is via GDF11 binding with TGF- β receptor on cell surface. To verify the role of VEGF from CM^{GDF11}, VEGF-neutralizing antibody was used to block VEGF in the conditioned medium (Supplemental Figure 11B), which resulted in significantly less tube formation of HUVECs (Supplemental Figure 11D), confirming that CM-secreted VEGF is responsible for the proangiogenesis effect. These findings indicated that one of GDF-11 functions in CMs is to promote angiogenesis via paracrine effect of on ECs.

To examine the possible direct effect of GDF-11 from CMs on ECs, rGDF-11 was used to treat ECs (Supplemental Figure 12A). Tube formation, proliferation, and migration of ECs were not significantly enhanced by external rGDF11 (Supplemental Figures 12A to 12C). These data suggest that GDF-11 had limited direct effect on ECs, and the paracrine effect of CM^{GDF11} on tube formation of ECs was primarily attributed to the expression of VEGF from CM^{GDF11}.

In addition to ECs, effect of CM^{GDF11} on cardiac fibroblasts was also examined. When neonatal mouse fibroblasts were treated with TGF- β 1, less fibrotic markers were expressed when the cells were cultured in the conditioned medium from CM^{GDF11} as compared with that from CM^{NC} (Supplemental Figure 13). These data indicated that overexpressed GDF-11 enhances paracrine action of CMs on the antifibrotic function of adjacent non-CMs.

GDF-11 DID NOT TRIGGER AND REVERSED MYOCYTE HYPERTROPHY BUT FUNCTIONED AS AN ENDOGENOUS SURVIVAL FACTOR.

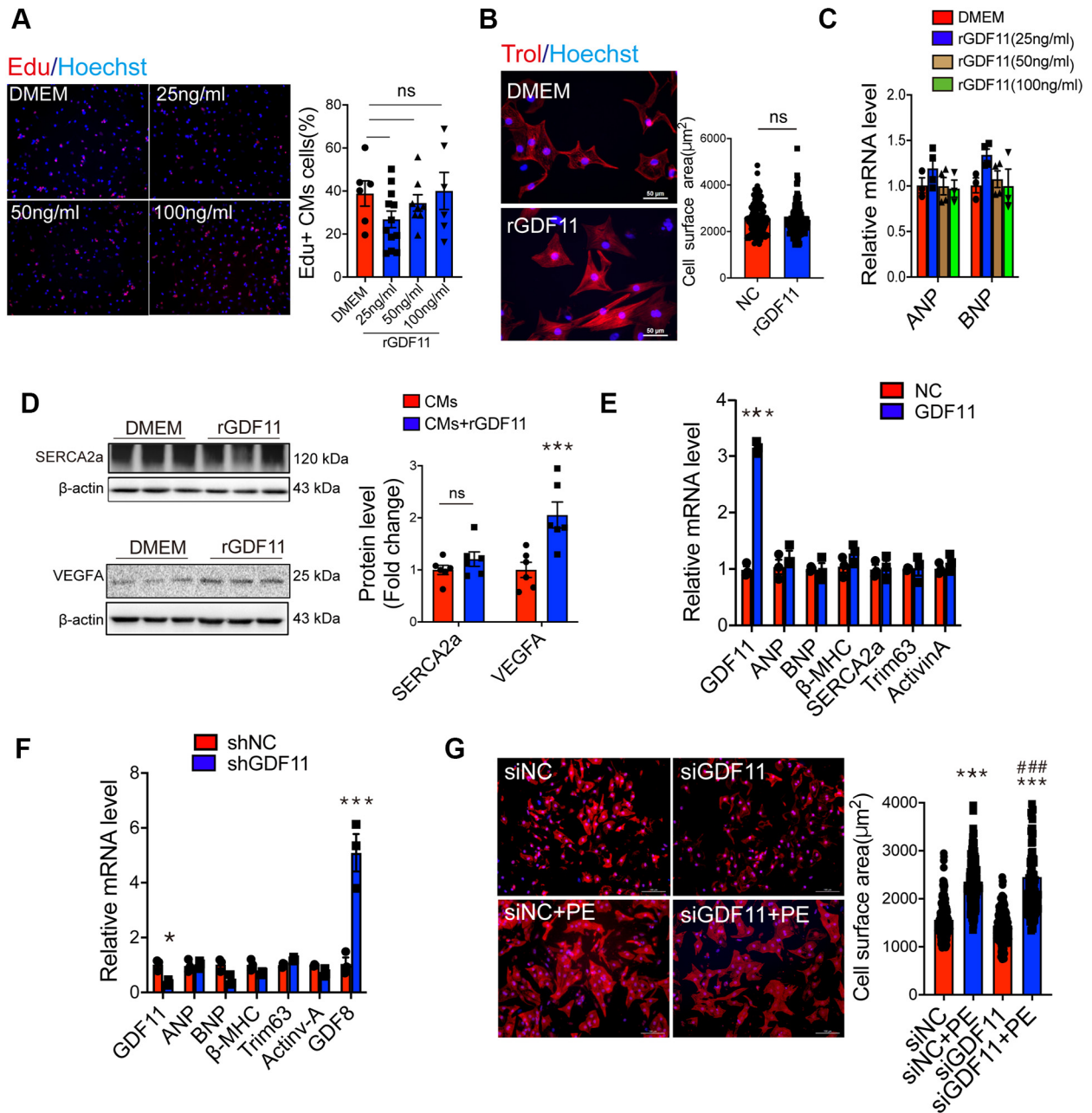
To study the autocrine effect of CM^{GDF11}, NMCMs were treated with rGDF-11. Different doses of rGDF-11 did not promote CM proliferation (Figure 5A). CMs pretreated with rGDF-11 were not larger (Figure 5B), nor did they have increased mRNA expression of ANP, and BNP as compared with the control CMs (Figure 5C). Similarly, there was no difference in the expression of SERCA2a between CMs treated with or without rGDF-11, but treatment of rGDF-11 induced more VEGF expression in CMs (Figure 5D). Consistent with this, quantitative polymerase chain reaction analysis demonstrated that either overexpression of GDF-11 or knockdown GDF-11 did not induce expression of classical marker

genes for hypertrophy in CMs, including ANP, BNP, β -myosin heavy chain, and SERCA2a, and Trim63 (a muscle atrophy-associated gene) (Figures 5E and 5F).

Neither GDF-11 overexpression nor knockdown in CMs affected PE-mediated hypertrophic growth of CMs (Figure 5G, Supplemental Figures 14A to 14C). However, conversely, overexpressed GDF-11 in CMs decreased the GDF-8 levels, and knockdown of GDF-11 increased GDF-8 (Supplemental Figure 14D). Activin A, another ligand of ActRIIB, and endogenous antagonists FSTL1 and FSTL3 in CMs were not affected by overexpressed GDF-11 (Supplemental Figure 14E). GDF-8 level in circulation was not changed in CKO mice compared with Cre with or without TAC surgery (Supplemental Figure 14F).

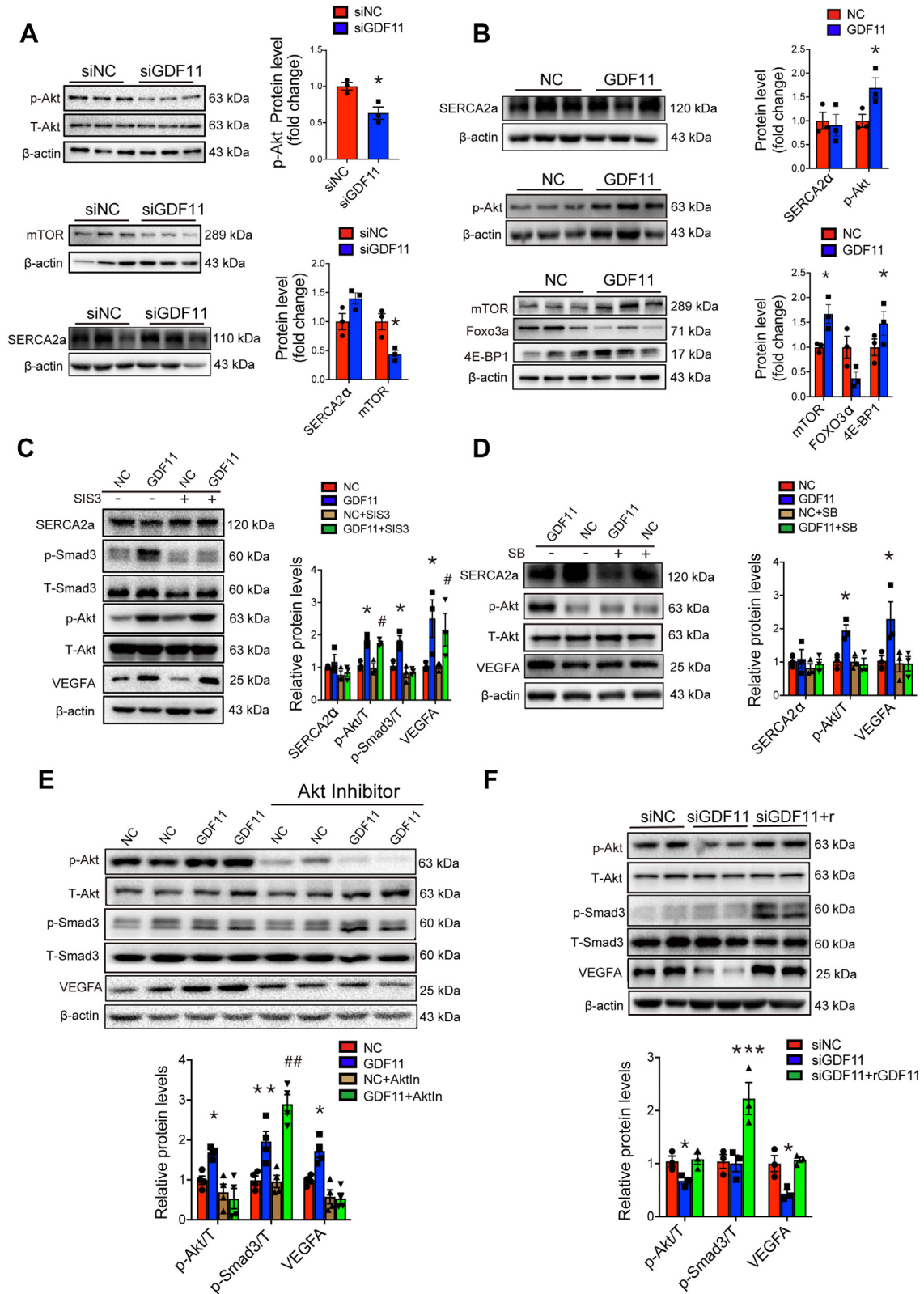
Given that GDF-11 did not reverse myocyte hypertrophy in vitro, it indicates that the protective effect of GDF-11 on heart observed in vivo study may be due to the myocardial paracrine effect of GDF-11 in CMs, and GDF-11 may act as the endogenous survival factor. Autophagy has been shown to be involved in CMs hypertrophic maladaptive process. Decreased expression of autophagosome marker LC3II and increased p62 levels were observed in CM^{GDF11} as compared with CM^{NC} under hypoxic conditions for inducing apoptosis (Supplemental Figure 15A), which suggested GDF-11 inhibited autophagy in CMs. On the other hand, knockdown GDF-11 in CMs (CM^{shGDF11}) increased LC3II expression compared with CM^{shNC} (Supplemental Figure 15B). The up-regulated LC3II levels in CM^{shGDF11} could be reduced to a level similar to the control CMs after CM^{shGDF11} transduced with lentiviral vector carrying GDF-11 (CM^{shGDF11+GDF11}) (Supplemental Figures 15C and 15D). Under electron microscopy, more vacuoles were found in CM^{shGDF11} as compared with control CM^{shNC}, confirming that knockdown GDF-11 induced more CMs apoptosis (Supplemental Figure 15E). Together, these results indicate that GDF-11 does not have pro- or anti-hypertrophic role in CM growth, but rather functioned as an endogenous survival factor.

EFFECT OF GDF-11 WAS VIA AKT/mTOR SIGNALING. The Akt signaling cascade is an important signaling pathway in the process of CM survival and angiogenesis. Knockdown of GDF-11 in NMCMs decreased the phosphorylation of both Akt and its downstream mTOR and had no significant effect on the expression of SERCA2a (Figure 6A). When CMs were cultured with rGDF-11, more phosphorylation of Akt in CMs was detected along with increased mTOR, as well as decreased expression of cell growth inhibitor FOXO3a (Figure 6B). Although activation of Smad transcription factors was considered as a traditionally

FIGURE 5 GDF11 Does Not Induce or Reverse Cardiac Hypertrophy, but Rather an Endogenous Protective Factor

(A) Representative images and percentage of Edu-positive CMs (indicated neonatal mouse CMs) after treatment with different doses of recombinant growth differentiation factor (GDF)-11 (25, 50, and 100 mg/µL) ($n = 6$ for Dulbecco's modified Eagle medium [DMEM] and 100 mg/µL, $n = 12$ for 25 mg/µL, $n = 8$ for 50 mg/µL). **(B)** Representative images of neonatal rat CMs (treated with 50 mg/µL rGDF11 or not) stained by troponin I (red) and DAPI (blue), and the quantification of cell surface area (scale bar = 50 µm) ($n > 10$ cells/group; $n = 10$). **(C)** Quantification of mRNA levels about cardiac hypertrophic markers (ANP and BNP) in neonatal mouse CMs after treatment with different dose of rGDF-11 (25, 50, and 100 mg/µL) ($n = 3$ for DMEM and 100 mg/µL, $n = 4$ for 25 mg/µL and 50 mg/µL). **(D)** Representative immunoblot and quantitation of SERCA2a and VEGFA proteins from neonatal mouse CMs after treatment with rGDF-11. β-actin was the loading control scenario ($n = 6$). *** $P < 0.001$ vs CMs. **(E)** Quantification of mRNA levels about GDF11, cardiac hypertrophic markers (ANP, BNP, β-MHC, SERCA2a), Trim63, and actin A in neonatal mouse CMs after transfection with LV-GDF-11 compared with LV-NC (NC) ($n = 3$). *** $P < 0.001$ vs NC. **(F)** Quantification of mRNA levels about GDF-11, cardiac hypertrophic markers (ANP, BNP, and β-MHC), Trim63 (a muscle atrophy-associated gene), and other members of the transforming growth factor β superfamily (actin A, GDF-8) in neonatal mouse CMs after transfection with shGDF11 compared with shNC ($n = 3$). * $P < 0.05$, *** $P < 0.001$ vs shNC. **(G)** Representative image of neonatal rat CMs transfected with siNC or siGDF-11 followed by PE 24 hours for inducing hypertrophy (scale bar = 20 µm). Quantification of the average cell surface area of CMs ($n > 20$ cells/group; $n = 6$). *** $P < 0.001$ vs siNC. ### $P < 0.001$ vs siGDF11. Abbreviations as in Figures 1, 2, and 4.

FIGURE 6 GDF-11 Alters Akt-mTOR Signaling Pathway Through Binding the Transforming Growth Factor β Type I Receptor in CMs



signal pathway of the TGF- β superfamily, SIS3 did not influence Akt activation and VEGF expression in CM^{GDF11}, while it inhibited phosphorylation of Smad3 (Figure 6C). These data suggested that Smad3 pathway was not linked with Akt activation after GDF-11 stimulation in CMs. However, when CM^{GDF11} were cultured with TGF- β receptor inhibitor SB431542, the expression of VEGFA and phosphorylated Akt (p-Akt) levels were all decreased (Figure 6D). Similarly, the paracrine action of GDF-11 in CMs was abolished by SB431542. The conditioned medium from CM^{GDF11} with SB431542 alleviated its effect on ECs tube formation (Supplemental Figure 11C). Treatment of CM^{GDF11} with an Akt inhibitor partially blocked the induction of VEGF expression (Figure 6E), indicating that the GDF-11-mediated proangiogenic effect is, at least partially, dependent on Akt activation. The decreased p-Akt and VEGF in CMs^{siGDF11} were also significantly rescued by addition of rGDF-11 into the culture (Figure 6F). Taken together, these data suggest that VEGF expression in CMs induced by GDF-11 partially depends on activation of Akt.

RESTORING GDF-11 EXPRESSION IN CMs RESCUED THE CARDIAC FUNCTIONS OF CKO MICE AFTER TAC. To study whether cardiac dysfunction in CKO mice after TAC can be rescued by restoring GDF-11 expression in the heart, CKO mice were injected intravenously with different doses (low, mild, and high) of an AAV9 vector carrying either the GDF-11 gene (AAV9-cTnT-GDF11) or with an empty vector (AAV9-Vec) before TAC surgery. GDF-11 was dose-dependently increased in the heart after AAV9-GDF-11 treatment (Supplemental Figures 16A and 16B), while no significant elevation of plasma GDF-11 was observed (Supplemental Figure 16C).

A mild dose of AAV9-GDF-11 treatment significantly improved the cardiac function of CKO mice to a level similar to Cre mice (Figure 7A). Hypertrophic CM size was reduced (Figure 7B) and capillary density was significantly increased (Figure 7C) in AAV-GDF-11-treated CKO mice after TAC as compared with the

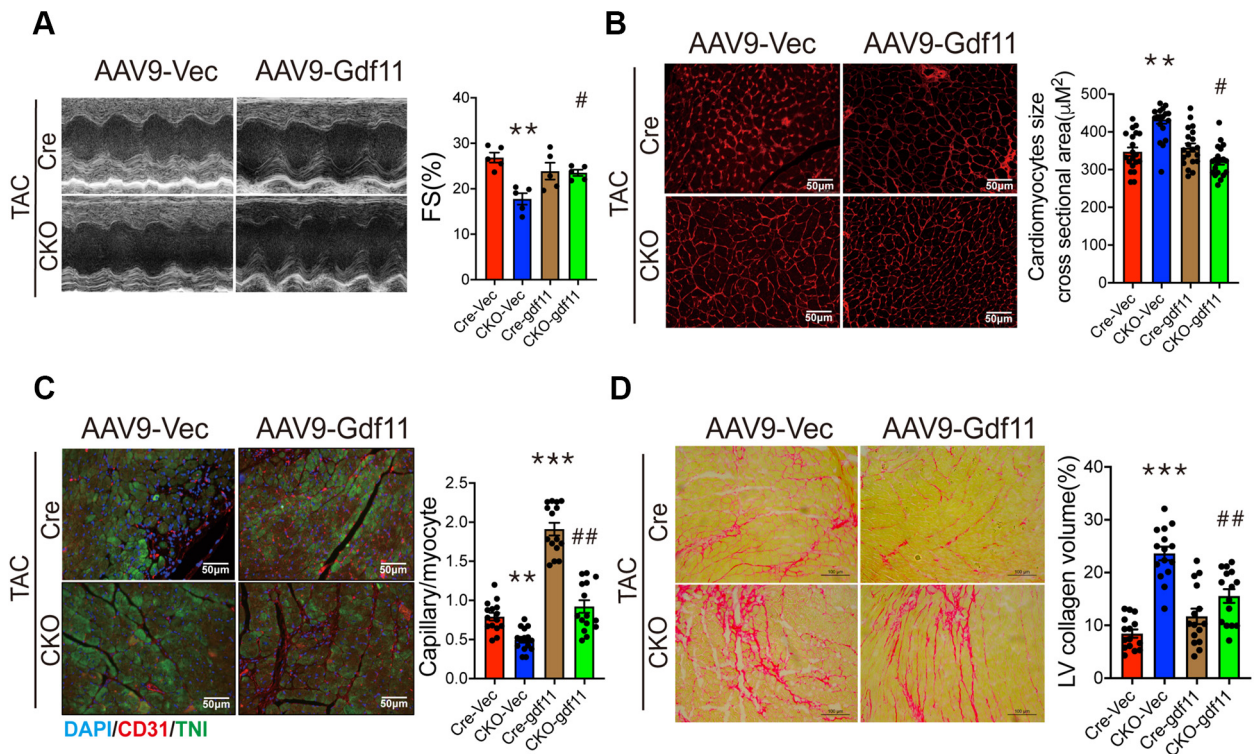
AAV9-Vec group. Cardiac fibrosis was also significantly reduced in AAV-GDF-11-treated mice after TAC compared with AAV9-Vec group (Figure 7D). AAV9-GDF-11 transduction with either a low or mild dose had an antifibrotic effect (Supplemental Figure 17A) and restored capillary density (Supplemental Figure 17B) in the heart in CKO mice 56 days after TAC. However, a high dose of AAV-9-mediated GDF-11 gene transfer in mice resulted in significant fibrosis in myocardium in both Cre and CKO mice as compared with nonoverexpressed Cre mice 56 days after TAC (Supplemental Figure 17A). Thus, moderate restoration of GDF-11 in CKO mice with AAV9 efficiently rescued the angiogenesis after TAC and preserved the cardiac function.

DISCUSSION

In this study, we found that GDF-11 in the heart was mainly from CMs and was induced by injury that promoted myocardial hypertrophy and heart failure (Figure 1). GDF-11 expression in the mouse heart after TAC changed dynamically from a significantly increased expression during hypertrophy to a gradually decreased expression during severe heart failure (Figure 1). Cardiac-specific knockout of GDF-11 at the embryonic and adulthood stages did not affect myocardial development and physiological growth (Figure 2). Neither overexpression nor knockdown of GDF-11 affected CM size or hypertrophy (Figure 5) but had protective effects on CMs (Supplemental Figure 17). These data demonstrate that GDF-11 is not essential for cardiac function under normal condition. However, deficiency of GDF-11 in CMs accelerated cardiac dysfunction after TAC, resulted in more severe left ventricular dilatation and more fibrosis, and caused quicker transition of cardiac hypertrophy into heart failure (Figure 3). This is in agreement with the latest study showing that targeted deletion of GDF-11 in CMs did not cause cardiac hypertrophy, but rather leads to left ventricular dilatation, suggesting a possible etiology for DCM.²⁶

FIGURE 6 Continued

(A) Representative immunoblot and quantification of phosphorylated Akt (p-Akt) and total Akt (T-Akt) and its downstream target mTOR, and SERCA2a levels in the CMs transfected with siRNA (siNC vs siGDF-11) (n = 3). *P < 0.05 vs siNC. (B) Immunoblot and quantification of SERCA2a, p-Akt, mTOR, FOXO3a, and 4E-BP1 levels in the CMs transfected with the null vector (NC) and LV-GDF-11 (n = 3). *P < 0.05 vs NC. (C) Immunoblot and quantification of SERCA2a, p-Smad3/T-Smad3, p-Akt/T-Akt, and VEGFA in CMs transfected with the null vector and LV-GDF-11 followed by treatment with Smad3 inhibitor (SIS3) (n = 3). *P < 0.05 vs NC. #P < 0.05 vs NC+SiS3. (D) Immunoblot and quantification of levels of p-Akt/T-Akt, SERCA2a, and VEGFA expression in CMs transfected with null-vector and LV-GDF11 followed by SB431542 (a transforming growth factor- β type I receptor inhibitor) (n = 3). *P < 0.05 vs NC. (E) Immunoblot and quantification of levels of p-Akt/T-Akt, p-Smad3/T-Smad3, and VEGFA in CMs transfected with the null vector and LV-GDF-11 followed by treatment with an Akt inhibitor (n = 4). *P < 0.05, **P < 0.01 vs NC. ###P < 0.01 vs NC+Akt inhibitor. (F) Immunoblot and quantification of levels of p-Akt/T-Akt, p-Smad3/T-Smad3, and VEGFA in CMs transfected with siRNA and followed by overexpressed LV-GDF-11 for 48 hours. β -actin was the loading control scenario (n = 4). CMs indicate primary neonatal mouse CMs. *P < 0.05, ***P < 0.001 vs siNC. Abbreviations as in Figures 1, 2, and 4.

FIGURE 7 GDF-11 Compensated by AAV9 Rescued the Cardiac Dysfunction in Knockout mice

(A) Representative images and quantification of echocardiographic FS of mice treated as described in the indicated groups ($n = 5$). **(B)** Representative images of WGA (scale bar = 50 μm) from the indicated groups after TAC. The quantification of average cross-sectional area of CMs in the indicated groups are shown in bar graph ($n = 20$). **(C)** Representative images of CD31 (red) from the indicated groups after TAC. The quantification of capillaries per CM in the indicated groups is shown in bar graph ($n = 15$). **(D)** Histological analyses of heart sections stained with Sirius red (scale bar = 100 μm) from the indicated groups after TAC ($n = 15$). ** $P < 0.01$, *** $P < 0.001$ vs Cre-Vec. # $P < 0.05$, ## $P < 0.01$ vs Cre-gdf11. AAV9 = adeno-associated virus serotype 9; TNI = troponin I; other abbreviations as in Figures 1, 2, and 4.

GDF-11 induced expression of paracrine factors like VEGF from CMs to promote cardiac angiogenesis by binding with the TGF- β receptor and activating its downstream Akt/mTOR signaling pathway (Figure 6). This is the first report describing the direct role and related mechanism of GDF-11 in myocardial development and pathology.

The roles of GDF-11 on cardiac functions are controversial.²⁷ GDF-11 could be either profibrotic or antifibrotic depending on the experimental setups/procedures. These controversies and dissimilarities could arise from using different in vitro and in vivo models with various GDF-11 delivery methods and dosages. Our data showed that GDF-11 expression was upregulated after TAC (Figure 1). Using an acute myocardial infarction mouse model, we found that GDF-11 was decreased in the heart after infarction (data not shown), which agreed with the current reports.²⁸ Such a difference in GDF-11 expression with different disease models at least partially explains the

current controversial status on the role of GDF-11 in cardiac functions.

It is known that the synthesis of hypertrophy-related proteins are increased during myocardial hypertrophy. Correspondently, angiogenesis in myocardium is also enhanced in order to maintain the supply of nutrition and oxygen for adaptation of the hypertrophic myocardium.²⁴ Accordingly, VEGF was increased during myocardial hypertrophy, which promoted angiogenesis.²⁰ When the formation of microvessels is disrupted, the normal structure and function of heart will be impaired, leading to heart failure. Our results show that when CMs were deficient in GDF-11, less VEGF was expressed and hypertrophy-induced angiogenesis was impaired, which resulted in more severe heart failure (Figure 3). This was confirmed by RNA-sequencing analysis showing that angiogenesis-related genes were the most impaired in CM^{shGDF11} (GEO:GSE182423) (Supplemental Figure 10). This agreed with the

previous report that blockage of VEGF led to lower blood vessel density and resulted in a rapid progression of hypertrophy to the decompensated stage of heart failure.^{20,25} Our study demonstrated that VEGF in CMs was induced by GDF-11. Enhanced GDF-11 expression in CMs increased the release of VEGF, whereas knockdown of GDF11 decreased VEGF expression and secretion (Figure 4). These data confirmed that GDF-11 regulated VEGF synthesis in CMs and played a positive role in the paracrine effect of CMs. This is also in line with our previous report that GDF-11 can induce VEGF expression in mesenchymal stem cells.²⁹

Because both GDF-11 and VEGF were increased and secreted from CM^{GDF11}, it was worthy to exclude the direct effect of GDF-11 on ECs. The effect of GDF-11 on ECs or angiogenesis has been studied by many groups, and results were controversial.^{18,30,31} We found that external rGDF11 did not affect ECs in aspects of proliferation, migration, and tube formation (Supplemental Figure 12). This is in consistent with previous reports³² suggesting that GDF-11 does not directly participate in proangiogenesis of ECs. It is worthy to point out that GDF-11 deficiency in ECs inhibited the proliferation and migration of ECs, which blocked progression of pulmonary hypertension, and thereby knockout of GDF-11 in ECs can reverse the phenotype of pulmonary hypertension (right ventricular hypertrophy).³¹ These results suggest that GDF-11 plays different roles in heart failure processes caused by different etiologies, especially in different cardiac cell types. However, our results reveal that the lack of GDF-11 in CMs could lead to a reduction of “cardiokines” from CMs and weaken CM communication with the endothelium. This suggests that GDF-11 is indispensable in proper communication between CMs and ECs in the heart for maintaining cardiac homeostasis and appropriate responsiveness to stress.

Until now, there were increasing controversies on the involvement of GDF-11 in fibrotic processes in various organ setups. Onodera et al³³ found that GDF-11 treatment of lung resident cells and lung fibroblast exposed to the cigarette smoke extract significantly inhibited cellular senescence and inflammation and significantly improved fibroblast-mediated tissue repair. Pons et al³⁴ found that marked prolonged GDF-11 treatment led to a progressive decline of a kidney mass, atrophy of the tubular epithelial cells, and increased fibrosis. Du et al³⁵ found in ischemia/reperfusion and myocardial infarction mice model, targeted delivery of GDF-11 in aged mice led to significant improvement of cardiac function and reduced infarct scar size formation

measured by Masson’s trichrome staining. Nonetheless, *in vitro* treatment of normal human fibroblast with GDF-11, GDF-8, or TGF- β significantly increased fibroblast activation in a dose-dependent manner. These results were consistent with data from Smith et al,¹¹ in which GDF-11 activated mouse embryonic fibroblasts (higher expression of collagen, α -smooth muscle actin, and vimentin) but to a lesser extent as observed in TGF- β -treated samples. In our case, we found that conditioned medium from CM^{GDF11} did not significantly promote transdifferentiation of fibroblasts and instead weakened the corresponding expression of fibrosis markers upon TGF- β 1 stimulation (Supplemental Figure 13). It is possible that there are other factors including VEGF from CMs playing the antifibrosis role.

The effect of GDF-11 on fibrosis is complex and probably depends on the organ and disease model. A superphysiological dose of GDF-11 could bring toxicity in tissue or organ. It is of importance to clarify the dose-response effect of GDF-11 in cardiac fibrosis. A high dose of AAV9-mediated GDF-11 gene transfer *in vivo* induced significant fibrosis in the myocardium in Cre mice (Supplemental Figure 17), while a mild dose of AAV9 vectors had an antifibrosis effect in the heart in CKO group after TAC. This demonstrated that cardiac dysfunction and fibrosis caused by GDF-11 deficiency in the heart could be rescued by moderate expression of GDF-11. If overexpression of GDF-11 by AAV9 in the heart significantly exceeds physiological dose, it will bring myocardial toxicity and lead to more obvious fibrosis in Cre and CKO mice. However, fibrosis in the Cre heart after injection of a high dose of AAV9-gdf11 had a lesser extent than in the CKO group. The overall side effects of overexpression of GDF-11 were inferior to those of knockout of GDF-11 in the heart under pressure overload, which indicated a significance of clinical translation to maintain balance of local concentration in heart tissue.

GDF-11 binds first to ActRII including ActRIIA and ActRIIB, and then recruits ActRI including ALK4, ALK5, and ALK7.³⁶ Binding GDF-11 with its receptors activates canonical Smad signaling pathways or noncanonical pathways, including the Akt and MAPK pathways. The serine/threonine protein kinase Akt is a key regulator of myocardial growth and paracrine effects that is essential for cardiac adaptation to diverse stress.³⁷⁻³⁹ In agreement with these reports, our data showed that overexpression of GDF-11 in CMs led to the up-regulation of Akt signaling and improved CM paracrine effects. Knockdown of GDF-11 led to a reduction in Akt phosphorylation and decreased secretion of VEGF (Figure 6A). Treatment

with an Akt inhibitor diminished the proangiogenic effect of GDF-11-treated CMs (Figure 6E). Although GDF-11 also activated canonical Smad2/3 pathway in CMs, the VEGF level of GDF-11-treated CMs was not attenuated by the SIS3 (Figure 6C). The paracrine effects and VEGF level of CMs^{GDF11} as well as phosphorylation of Akt could all be blocked by the TGF- β type I receptor inhibitor SB431542 (Figure 6D), confirming that the autocrine effect of GDF-11 was through binding with TGF- β receptor. Angiogenesis was enhanced during the acute phase of adaptive cardiac growth but reduced as hearts underwent pathological remodeling. GDF-11 deficiency in CMs impaired angiogenesis during the initial phase of heart growth and resulted in accelerated contractile dysfunction. Our data are consistent with that the enhanced angiogenesis in the acute phase of adaptive cardiac growth was associated with mTOR-dependent induction of myocardial VEGF.⁴⁰

Despite the similarities in sequence between mature GDF-8 and GDF-11,⁴¹ there are structural differences between the 2 proteins to distinguish their effects. Our findings of the deteriorating effect of GDF-11-deficient CMs are novel and different from previously described with CM-specific GDF-8 deletion.¹⁶ GDF-8 predominantly affects muscle mass, while the ablation of GDF-11 resulted in defects in skeletal patterning during embryogenesis, resulting in perinatal lethality.⁴² However, no cardiac developmental abnormality has been reported in GDF-8-null mice⁴³ as well as in our GDF-11 CM-null mice. CM-specific ablation of GDF-8 was reported to prevent cachexic changes, including muscle wasting and atrophy in heart failure, without alterations in cardiac function.⁴⁴ Heart-derived activin A also influences the cardiac cachexic states by acting on skeletal muscle in an endocrine manner.⁴⁵ These factors appear to function as endocrine hormones. In this study, cardiac-specific deletion of GDF-11 affect neither body weight nor the circulating GDF-11 levels, with no other organ abnormality. Interestingly, we found loss of GDF-11 lead to more GDF8 expression in CMs (Figure 5F), whereas overexpression of GDF-11 in CMs resulted in decreased GDF-8 (Supplemental Figure 14). Other groups also found increased cardiac mRNA expression of GDF-8 in cardiac-specific GDF-11-null mice,²⁶ which indicates the compensatory roles of between GDF-8 and GDF-11. In addition to GDF-8, activin A and endogenous antagonist FSTL1 and FSTL3 were not affected on the cellular level by GDF-11 (Supplemental Figure 14). Activin A and FSTL3 are cardiokines with opposing actions that function to regulate myocardial growth, fibrosis, and

the response to ischemic stress.⁴⁶ The physiological and pathological significances of these negative feedback regulations and cardiokine networks are still worthy to be explored further.

LIMITATIONS. Besides VEGF activation, we cannot deny the important role of other angiogenic factors in paracrine function of CMs. Screening for such secreted factors is worthy in a follow-up study. There was no change in circulating GDF-11 levels in the CKO mice (Supplemental Figure 6F), indicating that CMs are not the major source of circulating GDF-11 in mice. This also fits well with the fact that circulating GDF-11 level was unchanged in patients with heart failure or in the TAC mouse model. Our data are consistent with previous studies showing that the spleen was the major source of GDF-11 in circulation.⁷ All these results suggest that GDF-11 secreted from heart acts mainly locally and has less systemic effect as endocrine factors. It is worthy to explore the communication among different cell types within the heart and thereafter to develop a new therapeutic strategy and diagnostic markers for heart disease.

CONCLUSIONS

Cardiac-specific GDF-11-deficient mice exhibit exacerbation of cardiac dysfunction following pressure overload, whereas overexpression of GDF-11 results in diminished cardiac hypertrophic responses and improved function through enhancing angiogenesis via activating the Akt/mTOR pathway. The effect of cardiac GDF-11 belongs to local self-regulation of myocardial tissue, rather than to a systemic effect.

FUNDING SUPPORT AND AUTHOR DISCLOSURES

This work was supported by grants from the National Natural Science Foundation of China (Nos. 82070448, 81570251, and 81528002 to Dr Yu; No. 81670235 to Dr Yaping Wang) and the Youth Program of National Natural Science Foundation of China (No. 81902002 to Zhu, No. 81700424 to Dr Ma). The authors have reported that they have no relationships relevant to the contents of this paper to disclose.

ADDRESS FOR CORRESPONDENCE: Dr Hong Yu, Department of Cardiology, Second Affiliated Hospital, College of Medicine, Zhejiang University, Cardiovascular Key Laboratory of Zhejiang Province, 88 Jiefang Road, Hangzhou 310009, P.R. China. E-mail: yuvascular@zju.edu.cn. OR Dr Yaping Wang, Department of Cardiology, Second Affiliated Hospital, College of Medicine, Zhejiang University, Cardiovascular Key Laboratory of Zhejiang Province, 88 Jiefang Road, Hangzhou 310009, P.R. China. E-mail: yapingwang@zju.edu.cn.

PERSPECTIVES

COMPETENCY IN MEDICAL KNOWLEDGE: Factors secreted by the heart, referred to as “cardiokines,” have diverse actions in maintenance of cardiac homeostasis and remodeling, such as ANP, BNP, and GDF-15. Because the role of GDF-11 in cardiac diseases has not been fully determined, this study is to determine how endogenous GDF-11 exerts a functional role through autocrine and paracrine effects during the pathological process of cardiac hypertrophy. This study is the first to report that GDF-11 in the heart was mainly from CMs and that cardiac-specific knockout of GDF-11 at the embryonic and adulthood stages did not affect myocardial development and physiological growth. However, the lack of GDF-11

accelerated cardiac dysfunction after TAC via impairing angiogenesis. Moreover, moderate overexpression of GDF-11 in the heart may improve cardiac function and restore responsive angiogenesis, suggesting a clinical significance of GDF-11 in heart failure.

TRANSLATIONAL OUTLOOK: Lack of GDF-11 in the heart augmented the cardiac dysfunction induced by TAC via impairing angiogenesis. As overexpression of GDF-11 protects from cardiac dysfunction in response to pressure overload, we propose that rebalancing angiogenesis via GDF-11 local overexpression might be a promising therapeutic strategy to treat or prevent heart failure.

REFERENCES

- Nakamura M, Sadoshima J. Mechanisms of physiological and pathological cardiac hypertrophy. *Nat Rev Cardiol*. 2018;15:387-407.
- Shimizu I, Minamino T. Physiological and pathological cardiac hypertrophy. *J Mol Cell Cardiol*. 2016;97:245-262.
- Francis GS, Felker GM, Tang WH. A test in context: critical evaluation of natriuretic peptide testing in heart failure. *J Am Coll Cardiol*. 2016;67:330-337.
- Shimano M, Ouchi N, Walsh K. Cardiokines: recent progress in elucidating the cardiac secretome. *Circulation*. 2012;126:e327-e332.
- Zhao J, Pei L. Cardiac endocrinology: heart-derived hormones in physiology and disease. *J Am Coll Cardiol Basic Trans Science*. 2020;5:949-960.
- Nakashima M, Toyono T, Akamine A, Joyner A. Expression of growth/differentiation factor 11, a new member of the BMP/TGFbeta superfamily during mouse embryogenesis. *Mech Dev*. 1999;80:185-189.
- Loffredo FS, Steinhauser ML, Jay SM, et al. Growth differentiation factor 11 is a circulating factor that reverses age-related cardiac hypertrophy. *Cell*. 2013;153:828-839.
- Katsimpardi L, Litterman NK, Schein PA, et al. Vascular and neurogenic rejuvenation of the aging mouse brain by young systemic factors. *Science*. 2014;344:630-634.
- Sinha M, Jang YC, Oh J, et al. Restoring systemic GDF11 levels reverses age-related dysfunction in mouse skeletal muscle. *Science*. 2014;344:649-652.
- Egerman MA, Cadena SM, Gilbert JA, et al. GDF11 increases with age and inhibits skeletal muscle regeneration. *Cell Metab*. 2015;22:164-174.
- Smith SC, Zhang X, Zhang X, et al. GDF11 does not rescue aging-related pathological hypertrophy. *Circ Res*. 2015;117:926-932.
- Gaussin V, Depre C. Myostatin, the cardiac chalone of insulin-like growth factor-1. *Cardiovasc Res*. 2005;68:347-349.
- Jones JE, Cadena SM, Gong C, et al. Supraphysiologic administration of GDF11 induces cachexia in part by upregulating GDF15. *Cell Rep*. 2018;22:1522-1530.
- Jin Q, Qiao C, Li J, Li J, Xiao X. Neonatal systemic AAV-mediated gene delivery of GDF11 inhibits skeletal muscle growth. *Mol Ther*. 2018;26:1109-1117.
- Zimmers TA, Jiang Y, Wang M, et al. Exogenous GDF11 induces cardiac and skeletal muscle dysfunction and wasting. *Basic Res Cardiol*. 2017;112:48.
- Biesemann N, Mendler L, Wietelmann A, et al. Myostatin regulates energy homeostasis in the heart and prevents heart failure. *Circ Res*. 2014;115:296-310.
- Andersson O, Reissmann E, Ibáñez CF. Growth differentiation factor 11 signals through the transforming growth factor-beta receptor ALK5 to regionalize the anterior-posterior axis. *EMBO Rep*. 2006;7:831-837.
- Mei W, Xiang G, Li Y, et al. GDF11 Protects against endothelial injury and reduces atherosclerotic lesion formation in apolipoprotein E-null mice. *Mol Ther*. 2016;24:1926-1938.
- Hammers DW, Merscham-Banda M, Hsiao JY, Engst S, Hartman JJ, Sweeney HL. Supraphysiological levels of GDF11 induce striated muscle atrophy. *EMBO Mol Med*. 2017;9:531-544.
- Shen J, Xie Y, Liu Z, et al. Increased myocardial stiffness activates cardiac microvascular endothelial cell via VEGF paracrine signaling in cardiac hypertrophy. *J Mol Cell Cardiol*. 2018;122:140-151.
- O'Connell TD, Rodrigo MC, Simpson PC. Isolation and culture of adult mouse cardiac myocytes. *Methods Mol Biol*. 2007;357:271-296.
- Duran J, Troncoso MF, Lagos D, Ramos S, Marin G, Estrada M. GDF11 modulates Ca(2+)-dependent Smad2/3 signaling to prevent cardiomyocyte hypertrophy. *Int J Mol Sci*. 2018;19:1508.
- Sano M, Minamino T, Toko H, et al. p53-induced inhibition of Hif-1 causes cardiac dysfunction during pressure overload. *Nature*. 2007;446:444-448.
- Oka T, Akazawa H, Naito AT, Komuro I. Angiogenesis and cardiac hypertrophy: maintenance of cardiac function and causative roles in heart failure. *Circ Res*. 2014;114:565-571.
- Gogiraju R, Bochenek ML, Schäfer K. Angiogenic endothelial cell signaling in cardiac hypertrophy and heart failure. *Front Cardiovasc Med*. 2019;6:20.
- Garbern J, Kristl AC, Bassaneze V, et al. Analysis of Cre-mediated genetic deletion of Gdf11 in cardiomyocytes of young mice. *Am J Physiol Heart Circ Physiol*. 2019;317:H201-H212.
- Frohlich J, Vinciguerra M. Candidate rejuvenating factor GDF11 and tissue fibrosis: friend or foe? *GeroScience*. 2020;42:1475-1498.
- Li Z, Xu H, Liu X, et al. GDF11 inhibits cardiomyocyte pyroptosis and exerts cardioprotection in acute myocardial infarction mice by upregulation of transcription factor HOXA3. *Cell Death Dis*. 2020;11:917.
- Zhang C, Lin Y, Liu Q, et al. Growth differentiation factor 11 promotes differentiation of MSCs into endothelial-like cells for angiogenesis. *J Cell Mol Med*. 2020;24:8703-8717.
- Zhang J, Li Y, Li H, et al. GDF11 improves angiogenic function of EPCs in diabetic limb ischemia. *Diabetes*. 2018;67:2084-2095.

31. Yu X, Chen X, Zheng XD, et al. Growth differentiation factor 11 promotes abnormal proliferation and angiogenesis of pulmonary artery endothelial cells. *Hypertension*. 2018;71:729-741.
32. Zhang YH, Cheng F, Du XT, et al. GDF11/BMP11 activates both smad1/5/8 and smad2/3 signals but shows no significant effect on proliferation and migration of human umbilical vein endothelial cells. *Oncotarget*. 2016;7:12063-12074.
33. Onodera K, Sugiura H, Yamada M, et al. Decrease in an anti-ageing factor, growth differentiation factor 11, in chronic obstructive pulmonary disease. *Thorax*. 2017;72:893-904.
34. Pons M, Koniaris LG, Moe SM, Gutierrez JC, Esquela-Kerscher A, Zimmers TA. GDF11 induces kidney fibrosis, renal cell epithelial-to-mesenchymal transition, and kidney dysfunction and failure. *Surgery*. 2018;164:262-273.
35. Du GQ, Shao ZB, Wu J, et al. Targeted myocardial delivery of GDF11 gene rejuvenates the aged mouse heart and enhances myocardial regeneration after ischemia-reperfusion injury. *Basic Res Cardiol*. 2017;112:7.
36. Walker RG, Poggioli T, Katsimpardi L, et al. Biochemistry and biology of GDF11 and myostatin: similarities, differences, and questions for future investigation. *Circ Res*. 2016;118:1125-1141 [discussion: 1142].
37. Chaanine AH, Hajjar RJ. AKT signalling in the failing heart. *Eur Heart Fail*. 2011;13:825-829.
38. Fujio Y, Nguyen T, Wencker D, Kitsis RN, Walsh K. Akt promotes survival of cardiomyocytes in vitro and protects against ischemia-reperfusion injury in mouse heart. *Circulation*. 2000;101:660-667.
39. Abeyrathna P, Su Y. The critical role of Akt in cardiovascular function. *Vasc Pharmacol*. 2015;74:38-48.
40. Shiojima I, Sato K, Izumiya Y, et al. Disruption of coordinated cardiac hypertrophy and angiogenesis contributes to the transition to heart failure. *J Clin Invest*. 2005;115:2108-2118.
41. Walker RG, Czepnik M, Goebel EJ, et al. Structural basis for potency differences between GDF8 and GDF11. *BMC Biol*. 2017;15:19.
42. McPherron AC, Lawler AM, Lee SJ. Regulation of anterior/posterior patterning of the axial skeleton by growth/differentiation factor 11. *Nat Genet*. 1999;22:260-264.
43. Heineke J, Auger-Messier M, Xu J, et al. Genetic deletion of myostatin from the heart prevents skeletal muscle atrophy in heart failure. *Circulation*. 2010;121:419-425.
44. Rausch V, Sala V, Penna F, Porporato PE, Ghigo A. Understanding the common mechanisms of heart and skeletal muscle wasting in cancer cachexia. *Oncogenesis*. 2021;10:1.
45. Lee SJ, Lee YS, Zimmers TA, et al. Regulation of muscle mass by follistatin and activins. *Mol Endocrinol*. 2010;24:1998-2008.
46. Oshima Y, Uchi N, Shimano M, et al. Activin A and follistatin-like 3 determine the susceptibility of heart to ischemic injury. *Circulation*. 2009;120:1606-1615.

KEY WORDS angiogenesis, cardiac hypertrophy, GDF-11, fibrosis, heart failure

APPENDIX For an expanded Methods and References sections as well as supplemental tables and figures, please see the online version of this paper.